Supporting Information for
Chain dynamics and nanoparticle motion in attractive polymer nanocomposites subjected to large deformations

Erkan Senses[1,2], Madhusudan Tyagi[1,2], Bharath Natarajan[3], Suresh Narayanan[4], Antonio Faraone[1]

[1]*NIST Center for Neutron Research, National Institute of Standards and Technology Gaithersburg, MD 20899-8562 USA*
[2]*Department of Materials Science and Engineering, University of Maryland College Park, MD 20742-2115 USA*
[3]*Materials Measurement Laboratory, National Institute of Standards and Technology Gaithersburg, MD 20899 USA*
[4]*Advanced Photon Source, Argonne National Laboratory, Argonne, IL 60439 USA*

e-mail address: erkan.senses@nist.gov & antonio.faraone@nist.gov

I. Small-angle neutron scattering (SANS)

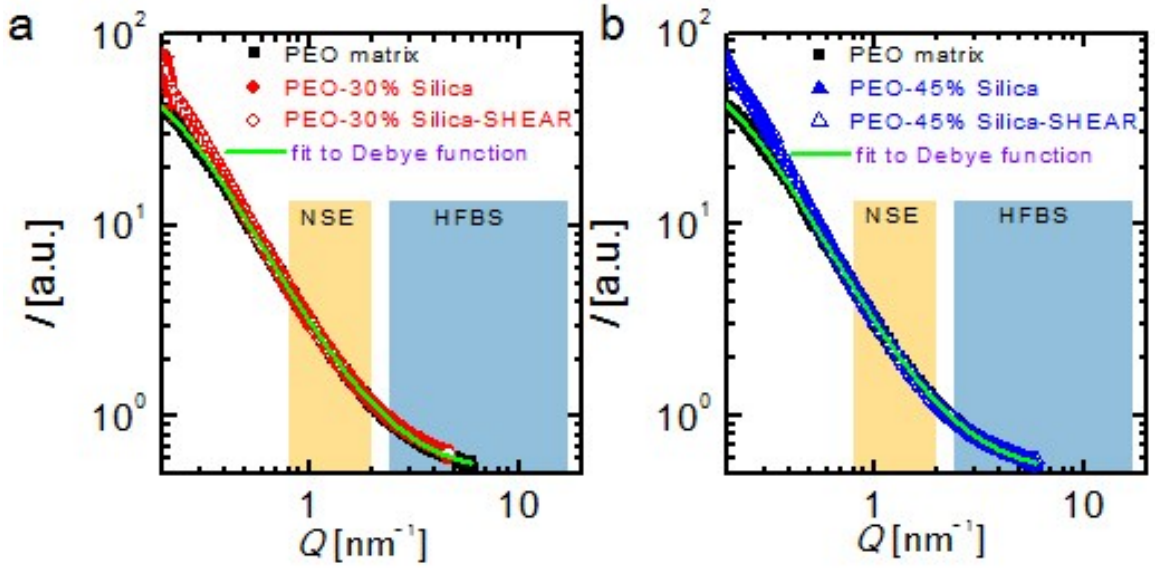

FIG. S1. SANS profiles from PEO homopolymer and nanocomposites with d/h (52/48) PEO matrix (zero-average contrast matched) and (a) 30 % Silica, (b) 45 % Silica before and after shear. The shaded regions show the *Q*-ranges used for neutron spin echo (NSE) and neutron backscattering (HFBS). The green lines are the Debye functions fit of the homopolymer data.

SANS experiments were performed at NGB30SANS beamline at the NIST Center for Neutron Research (NCNR, Gaithersburg, MD). Samples sandwiched between quartz windows were melted under vacuum at 363 K (above the melting temperature of PEO, $T_{m,PEO} \approx 338$ K) for 15 min and then tightened to obtain

the final thicknesses of ≈ 0.1 mm. All scattering profiles were corrected for background, empty cell and sample transmission to get 1-D isotropic scattering patterns. SANS profiles from PEO homopolymer and Silica nanocomposites with d/h (52/48) PEO matrix are shown in Figure S2. The profiles are identical in the NSE and HFBS Q-range, indicating the absence of significant scattering from the particles in this Q range.

II. Quasielastic neutron scattering (QENS)

a) QENS spectra at $Q = 3.6$ nm^{-1}

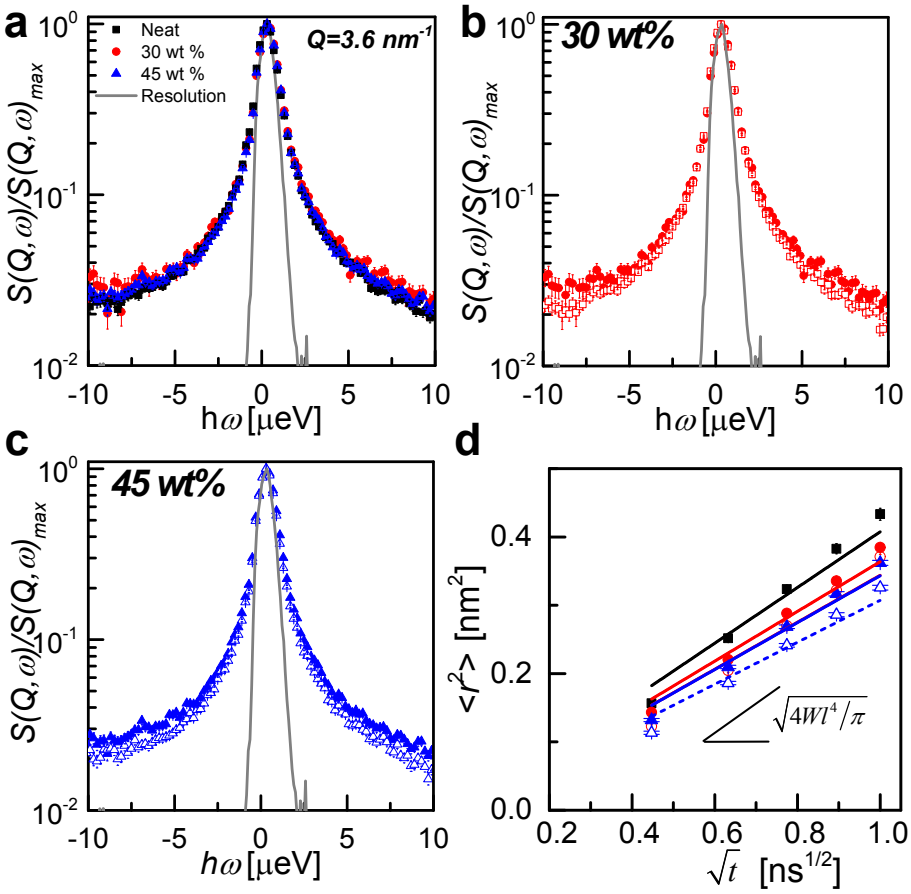

FIG. S2. Incoherent dynamic structure factors obtained in neutron backscattering at $Q = 3.6$ nm^{-1} for **(a)** neat PEO and the composites with a mass fraction of 30 % and 45 % SiO_2 and PEO without large shear. Dynamic structure factors before (filled symbols) and after (open symbols) large shear are compared for the **(b)** 30 % and **(c)** 45 % samples. **(d)** Mean-square displacement (MSD) obtained from the Inverse-Fourier transformed backscattering data plotted on Rouse scaling ($t^{0.5}$). The solid and dashed lines are the best fits to unsheared and sheared samples, respectively.

b) QENS analysis in the energy domain

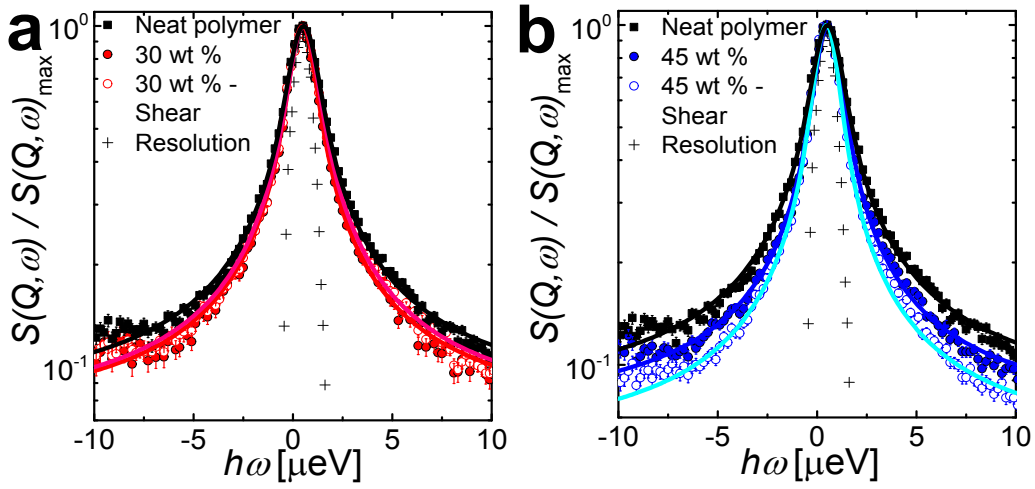

FIG. S3. Incoherent dynamic structure factors obtained in neutron backscattering at $Q = 4.7$ nm^{-1} for neat PEO and the composites with a weight fraction of 30 % and 45 % SiO_2 before and after large shear. The fits are the best fit of the data to Fourier transformed-KWW function convoluted with the experimental resolution and using exponent, β=0.5, valid for Rouse scaling.

To verify that our results are not influenced by the method of analysis we also fitted the HFBS data in the energy domain using the Fourier transform of a KWW function.

Table S1. Characteristic Rouse rates *(Wl⁴)* of PEO at *T*=363 K determined as the average of the results from fitting of Fourier transformed KWW function to the dynamic structure factor *S(Q, ω)* at Q = (3.6 and 4.7) nm^{-1}.

Sample	***Wl⁴*** (from fitting to KWW) **[nm⁴/ns]**
Neat PEO	0.209 ± 0.004
PEO-30 wt % SiO_2	0.193 ± 0.005
PEO-30 wt % SiO_2-SHEAR	0.196 ± 0.004
PEO-45 wt % SiO_2	0.173 ± 0.003
PEO-45 wt % SiO_2-SHEAR	0.156 ± 0.003

Note that the trends found with the analysis in the energy domain are similar to those obtained in the time domain discussed in the main text. The larger numbers found in the former could be explained by the fact

that the KWW fits were applied to the full energy range of the spectra whereas in the time domain we restricted the analysis below 1 ns where the Rouse scaling applied (mean-squared-displacement $\propto t^{0.5}$).

c) Coherent contribution

From the fitting of the SANS data (Figure S1), we first estimated the coherent and incoherent (background) contribution to the total scattering at Q = (3.6 and 4.7) nm^{-1} as 30% and 20 %, respectively. We then calculate the coherent Rouse intermediate scattering functions at these Q values with the following equation using the obtained Wl^4 :

$$S_{Rouse}(Q,t) = \frac{1}{N}\sum_{m,n}^{N}\left\{\exp(-Q^2 D_R t - \frac{1}{6}|m-n|Q^2 l^2) - \frac{2}{3}\frac{R_e^{\,2}Q^2}{\pi^2}\sum_{p=1}^{N}\frac{1}{p^2}\cos(\frac{p\pi m}{N})\cos(\frac{p\pi n}{N})[1-\exp(\frac{-p^2 t}{\tau_R})]\right\}$$

Here $R_e = \sqrt{Nl^2}$ is end to end distance of a single chain, $D_R = Wl^4/(3R_e^{\,2})$ is the Rouse diffusion coefficient, $\tau_R = N^2/(\pi^2 W)$ is the Rouse time and N is the degree of polymerization.

Fitting these curves using the model function for the incoherent Rouse dynamics, $S_{Rouse}(Q,t) = \exp[-\frac{Q^2}{6} < r^2(t) >]$ with $< r^2(t) >= \sqrt{4Wl^4 t/\pi}$, values of Wl^4 overestimated by a factor of three are obtained. Thus, by a weighted sum of the coherent and incoherent contributions to the total scattering, we calculate that the Wl^4 values obtained from the HFBS data are overestimated by 60 % and 40 % at Q=3.6 nm^{-1} and at 4.7 nm^{-1}, respectively. This finding, however, does not affect our comparison between the different samples because the SANS pattern, and thus the relative weight of the coherent and incoherent contributions, does not change between the different samples or after shear.

III. X-ray photon correlation spectroscopy (XPCS) and small-angle x-ray scattering (SAXS)

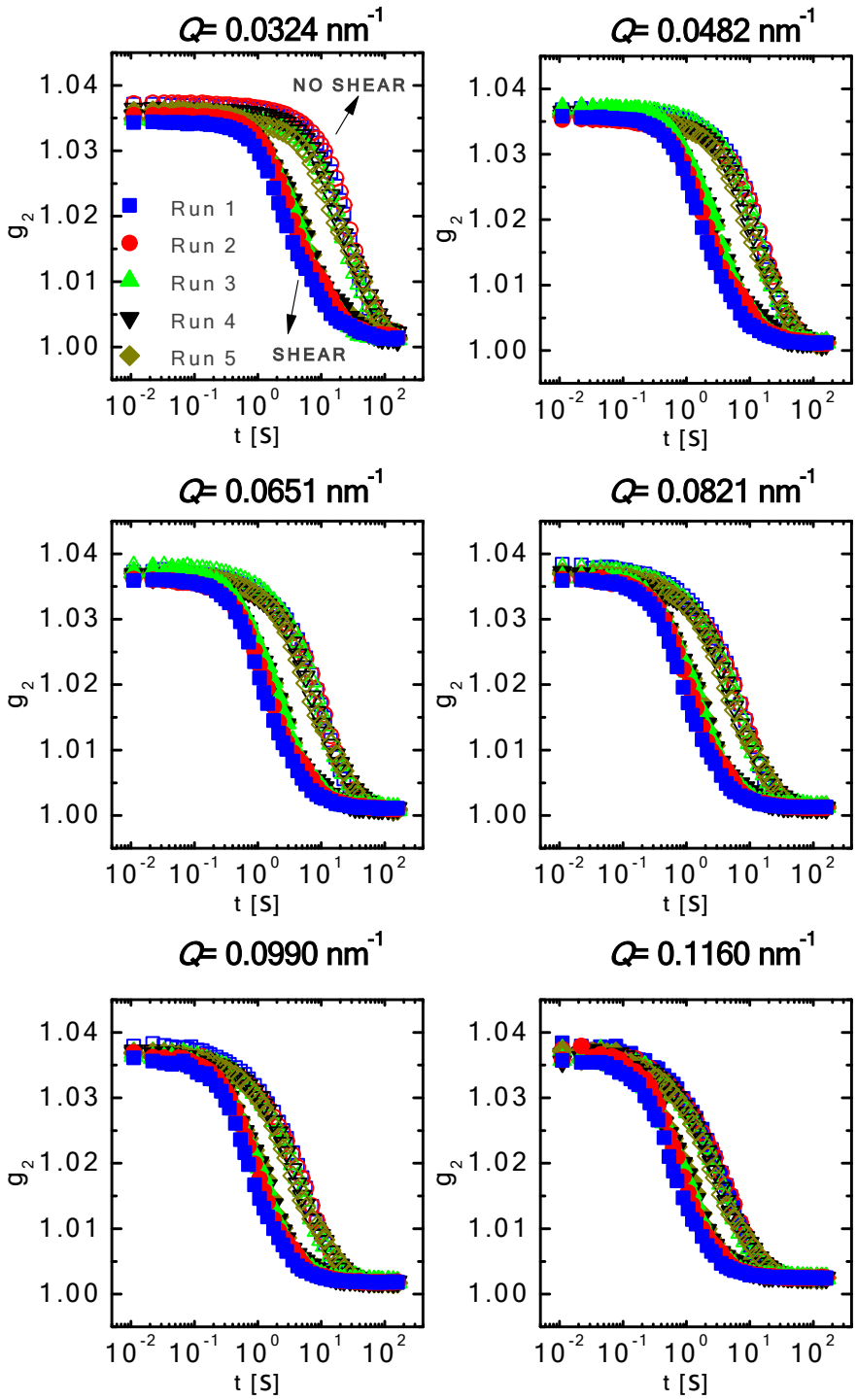

FIG. S4. The Q-dependent intensity-intensity autocorrelation functions for sheared and unsheared samples collected in five subsequent runs confirming the homogenous particle distribution and the absence of radiation damage.

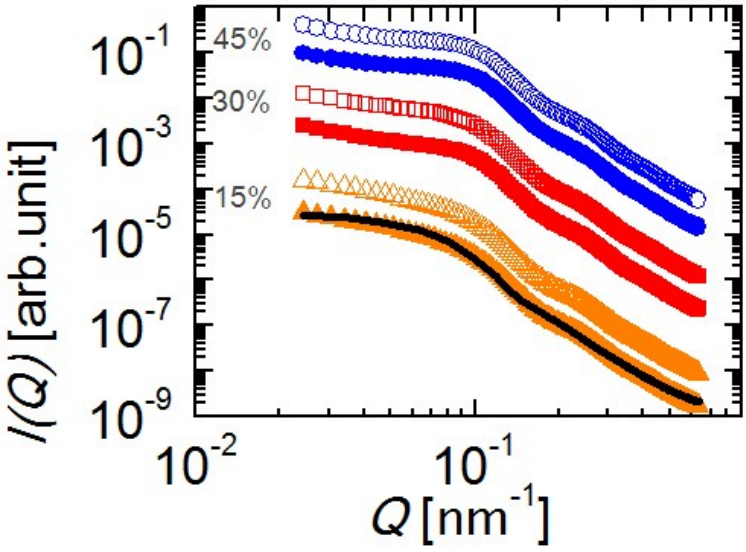

FIG. S5. The SAXS profiles of unsheared (filled symbols) and sheared (open symbols)) nanocomposite samples (circles). The line shows the sphere form factor with particle average radius of 24 nm and polydispersity 0.3. The curves are shifted vertically for clarity.